Articles

Effects of Cholesterol and Enantiomeric Cholesterol on P-Glycoprotein Localization and Function in Low-Density Membrane Domains†

Gary D. Luker,‡,§ Christina M. Pica,‡,§ A. Sampath Kumar,§ Douglas F. Covey,§ and David Piwnica-Worms*,‡,§

Laboratory of Molecular Radiopharmacology, Mallinckrodt Institute of Radiology, and Department of Molecular Biology and Pharmacology, Washington University School of Medicine, St. Louis, Missouri 63110

Received December 13, 1999; Revised Manuscript Received March 27, 2000

ABSTRACT: Multidrug resistance P-glycoprotein (Pgp) has been reported to localize in low-density, cholesterol-enriched membranes. However, effects of low-density membrane domains on function of Pgp remain unexplored in whole cell systems. In cells that express modest levels of the protein endogenously or through drug selection, Pgp predominantly localized to low-density membranes following separation on a sucrose gradient. When highly overexpressed in NIH 3T3 cells, a prominent amount of Pgp also was detected in high-density membranes. Removing cholesterol from cells with β-methylcyclodextrin (CD), a sterol acceptor molecule, shifted fractions that contained Pgp from low toward high density, and this effect was reversed to a similar extent by restoring sterols with either cholesterol or enantiomeric cholesterol. However, function of human *MDR1* Pgp as probed with Tc-Sestamibi, a transport substrate for Pgp, was not dependent on localization of Pgp in cholesterol-enriched membranes. Specific inhibition of *MDR1* Pgp with GF120918 or LY335979 also was independent of cholesterol. Cell-type-specific effects of cholesterol content on function of human Pgp were detected by use of daunomycin, another substrate for Pgp, although efficacy of inhibitors remained independent of cholesterol. Conversely, both function and inhibition of hamster Pgp as measured with Tc-Sestamibi and daunomycin were in part dependent on normal cell content of cholesterol. These data show that Pgp preferentially localizes to low-density, cholesterol-enriched membrane domains, but acute depletion of cholesterol impacts Pgp-mediated drug transport in a substrate- and cell-type-specific manner.

MDR1 P-glycoprotein (Pgp)[1] is an approximately 170 kDa protein that is a member of the ABC superfamily of membrane proteins. When expressed in tumor cells, *MDR1* Pgp and other class I Pgps (*mdr*1 and *mdr3* in mice, *pgp*1 and *pgp2* in hamsters) confer resistance to structurally and functionally diverse chemotherapeutic drugs by decreasing intracellular concentrations of these compounds (for recent reviews, see (refs *1*−*3*). However, the molecular mechanisms of *MDR1* Pgp remain under investigation (*4*). Pgp has been proposed to function as a flippase for lipids and drugs (*5*), a "vacuum cleaner" for extracting hydrophobic compounds from within the lipid bilayer (*6*), or a regulator of electrochemical potential (*1*).

MDR1 Pgp is present normally in many different tissues, including liver, kidney, adrenal, epithelia of the choroid plexus and intestine, and capillary endothelial cells at the blood−brain barrier (*7*, *8*). In polarized cells, Pgp is localized to apical membranes, domains that are enriched in sphingolipids and cholesterol compared with basolateral surfaces (*9*, *10*). *MDR1* Pgp has been proposed to function in several different aspects of normal physiology (*4*), including protection from xenobiotics (*11*), resistance to apoptosis (*12*, *13*), migration of dendritic cells into lymphatic vessels (*14*), and intracellular trafficking of sterols (*15*−*18*). Nevertheless, the role of *MDR1* Pgp in normal cells and the relationship of physiologic function(s) to multidrug resistance (MDR) remain uncertain.

Lipids exert complex effects on class I Pgp in a variety of experimental systems. In isolated canalicular vesicles from rat liver, increases in membrane fluidity with compounds such as benzyl alcohol inhibit ATP-dependent accumulation of daunomycin and vinblastine, two drugs that are in the MDR phenotype (*19*). Photoaffinity labeling of Pgp in membranes and ATPase activity of the protein in proteoliposomes also are inhibited by agents that increase membrane fluidity (*20*). Maintenance of a lipid−protein interface is

† This work was supported by U.S. Department of Energy Grant DE-FG02-94ER61885 (D.P-W.), National Institutes of Health Grant GM47696 (D.F.C.), and Mentored Clinical Scientist Career Development Award K08 HL03683 (G.D.L.).

* To whom correspondence should be addressed at the Mallinckrodt Institute of Radiology, 510 S. Kingshighway Blvd., St. Louis, MO 63110. Tel 314-362-9356; fax 314-362-0152; e-mail piwnica-wormsd@mir.wustl.edu.

‡ Laboratory of Molecular Radiopharmacology, Mallinckrodt Institute of Radiology.

§ Department of Molecular Biology and Pharmacology.

[1] Abbreviations: ABC, ATP-binding cassette; BSA, bovine serum albumin; CD, β-methylcyclodextrin; CHO, Chinese hamster ovary; DMSO, dimethyl sulfoxide; ent-cholesterol, (3α,8α,9β,10α,13α,14β,17α,20*S*)-cholest-5-en-3-ol; MDR, multidrug resistance; Pgp, P-glycoprotein; PBS, phosphate-buffered saline.

10.1021/bi9928593 CCC: $19.00
Published on Web 06/07/2000

essential to prevent inactivation of Pgp during purification (*21*), and function of Pgp in reconstituted systems is altered by lipid composition. By use of Pgp in proteoliposomes, photoaffinity labeling with azidopine is stimulated optimally by 20% cholesterol in the lipid mixture, while binding decreases with greater concentrations of cholesterol (*22*). The yeast sterol ergosterol inhibits photoaffinity labeling of Pgp in proteoliposomes and inactivates the protein in a heterologous expression system, demonstrating that ergosterol cannot substitute effectively for cholesterol in these assays of Pgp (*22*, *23*). ATPase activity of Pgp in proteoliposomes also is affected by phospholipids. Under basal conditions, ATPase activity differs in proteoliposomes formed from sheep brain, bovine liver, or *Escherichia coli* lipids; stimulation of ATP hydrolysis in response to drugs is not observed when lipids from *Escherichia coli* are used (*24*). Using hamster Pgp, Romsicki and Sharom (*25*) show that stimulation and inhibition of ATPase activity in response to verapamil differed in liposomes composed of egg phosphatidylcholine, dimyristoylphosphatidylcholine, or dipalmitoylphosphatidylcholine. However, ATPase activity in response to vinblastine or daunorubicin is not affected by changes in lipid composition. Although these reports demonstrate that class I Pgp is affected significantly by lipids, few studies have used intact cells to analyze effects of lipids on the reduced accumulation of drugs mediated by Pgp.

Recent studies have shown that a significant proportion of class I Pgp is present in low-density membranes separated on sucrose gradients (*26*, *27*). Such localization is consistent with expression of Pgp on the apical surface of polarized cells, because both apical membranes and low-density membrane fractions are relatively enriched in sphingolipids and cholesterol (*9*, *28*). Using drug-selected CH^RC5 cells, Demeule et al. (*27*) also demonstrated that the proportion of Pgp fractionating with low-density membranes increases when cells are cultured in the presence of substrates for Pgp, compared with cells that are grown in the absence of drug. However, effects of Pgp localization to low-density, cholesterol-enriched membranes on transport function have not been investigated.

To analyze the effect of cholesterol on localization and function of Pgp in membrane domains, we used a detergent-free extraction procedure to identify Pgp in fractions from sucrose gradients. Cells with endogenous Pgp were compared with cell lines that express *MDR1* Pgp by drug selection or transfection. Depletion of cellular cholesterol with the sterol acceptor β-methylcyclodextrin (CD) was analyzed by shifts in density of membrane fractions in which Pgp was detected. We then quantified effects of cholesterol depletion on function of Pgp as probed with two different transport substrates and specific modulators of the protein. In addition, we determined the relative effects of restoring cellular sterols with either cholesterol or the synthetic enantiomer of cholesterol [(3α,8α,9β,10α,13α,14β,17α,20*S*)-cholest-5-en-3-ol] (ent-cholesterol) on fractionation and function of class I Pgp. Results showed that Pgp localized primarily to low-density membrane domains in cells that express physiologic amounts of the protein, while Pgp also was identified in high-density fractions from cells that overexpress the protein. Depletion of cellular cholesterol shifted the fractions that contained Pgp to higher density on sucrose gradients, an effect that was reversed to a similar extent with either cholesterol or ent-cholesterol. However, cell-type- and substrate-specific effects on the function of class I Pgp were observed.

MATERIALS AND METHODS

Materials. Stock solutions of GF120918 (gift of Glaxo-Wellcome) and LY335979 (gift of Eli Lilly and Co.) were prepared in dimethyl sulfoxide (DMSO). Synthesis of (3α,8α,9β,10α,13α,14β,17α,20*S*)-cholest-5-en-3-ol, the enantiomer of cholesterol, was performed as described previously (*29*). β-Methylcyclodextrin (CD) and fatty-acid deficient bovine serum albumin (BSA) were from Sigma. [^{99m}Tc]-Sestamibi was prepared with a one-step kit formulation (Cardiolite, Du Pont Medical Products Division) (*30*). [^{3}H]-Daunomycin (1.9 Ci/mmol) was obtained from DuPont NEN. All other reagents were from Sigma.

Cell Culture and Buffers. NIH 3T3 fibroblasts were grown in DMEM, 10% heat-inactivated calf serum, and 0.1% penicillin/streptomycin. NIH 3T3 cells stably transfected with human *MDR1* (obtained from Michael Gottesman, NIH) were maintained in 60 ng/mL colchicine. Human HepG2 and KB 3-1 cell lines were cultured in DMEM, 10% heat-inactivated fetal bovine serum, 1% L-glutamine, and 0.1% penicillin/streptomycin. The derivative KB 8-5 cell line was maintained in 10 ng/mL colchicine. Chinese hamster ovary (CHO) K1 cells were grown in F-12 with 5% heat-inactivated calf serum, 1% L-glutamine, and 0.1% penicillin/streptomycin. Human 8226 myeloma cells and the doxorubicin-selected derivative Dox6 cell line (gift of William Dalton, Moffitt Cancer Center) were grown in suspension culture as described previously (*31*). All cells were maintained in a 5% CO_2 incubator at 37 °C. Control buffer for assays of radiotracer accumulation was a modified Earle's balanced salt solution (MEBSS) containing the following millimolar concentrations: 145 Na^+, 5.4 K^+, 1.2 Ca^{2+}, 0.8 Mg^{2+}, 152 Cl^-, 0.8 $H_2PO_4^-$, 0.8 SO_4^{2-}, 5.6 dextrose, 4.0 HEPES, and 0.1% fatty-acid deficient BSA (w/v), pH 7.4. Sucrose gradients were prepared in MES-buffered saline (25 mM MES, pH 6.5, 150 mM NaCl, and 2 mM EDTA) (*32*).

Synthesis of Sterol−CD Complexes. Complexes of cholesterol or ent-cholesterol with CD were prepared as described by Klein et al. (*33*).

Treatment of Cells with CD and Sterol−CD Complexes. All incubations and washes were performed with serum-free medium. Cells were washed with the appropriate medium and then incubated with 15 mM CD for 30 min to deplete cholesterol. For experiments evaluating repletion of cellular cholesterol following treatment with CD, cells were washed and then incubated for 60 min in medium containing 0.2 mM sterol−CD complex. To load cells with cholesterol or ent-cholesterol without prior CD treatment, cells were washed and incubated for 60 min in medium with 0.2 mM sterol−CD complex. Control cells were incubated in medium alone. All incubations with CD and sterol−CD complexes were performed at 37 °C in a 5% CO_2 incubator.

Fractionation of Cells on Sucrose Gradients. Cells were plated at a density of (3−3.5) × 10^5 cells/10-cm dish and cultured in normal medium for 3 days. Following treatment with CD and/or sterol−CD complex as described, cells were washed three times in PBS. Cells from three (NIH 3T3 *MDR1*), four (KB 8-5, CHO), or five (HepG2) 10-cm dishes

were pooled for detergent-free fractionation of low-density membrane domains on discontinuous sucrose gradients (5%, 35%, and 40% steps) as described by Pike and Miller (*32*). Because HepG2 cells express low amounts of Pgp, membrane-associated proteins in each fraction were concentrated with minor modifications of the method described by Roy et al. (*34*). Briefly, 0.8 mL from each sucrose fraction was diluted to a final volume of 15 mL with MES-buffered saline and centrifuged at 100000*g* for 1 h in a 70Ti rotor (Beckman). Pellets were then resuspended in 125 μL of MES-buffered saline for analysis.

Immunofluorescence Microscopy. HepG2 cells were grown on glass cover slips as described above and processed for immunofluorescence microscopy with mAb C219 (Signet) as previously described by our laboratory, except that propidium iodide was not used in the mounting medium (*8*). Similarly, KB 8-5 and CHO cells were grown and processed for immunofluorescence microscopy with the following minor modifications to the protocol: (1) PBS with 5% horse serum and 1% BSA was used for blocking and dilution of antibodies; (2) blocking was performed for 1 h before application of mAb C219; and (3) PBS with 1% BSA was used for washing cover slips before incubation with the secondary antibody.

Western Blots. Aliquots (100 μL) of each fraction from sucrose gradients or HepG2 pellets were separated on a 7% gel by SDS−PAGE. Pgp was detected by Western blotting with mAb C219 as described previously (*35*).

Cellular Accumulation of [^{99m}Tc]Sestamibi or [^{3}H]Daunomycin. Cells were grown on cover slips as described above, except for 8226 cell lines that were maintained in suspension culture. After the appropriate treatment with CD and/or sterol−CD complex, assays of transport function and inhibition of class I Pgp with [^{99m}Tc]Sestamibi (1.5 μCi/mL) or [^{3}H]daunomycin (0.2 μCi/mL) were performed as described previously by our laboratory (*30*, *36*). Control experiments showed that background radioactivity in all assays did not differ among treatments with medium, CD, or sterol−CD complexes. Cell contents are reported as femtomoles of Tc-Sestamibi (milligram of protein)$^{-1}$ $(nM_o)^{-1}$ or picomoles of daunomycin (milligram of protein)$^{-1}$ $(\mu M_o)^{-1}$, where $(nM_o)^{-1}$ and $(\mu M_o)^{-1}$ represent total concentration of tracer in the extracellular buffer.

Lipid Analysis. Following treatment of cells with CD and/or sterol−CD complexes as described above, cells were washed with PBS and lipids were extracted with hexane/2-propanol (3:2 v/v) for 1 h. Cells were then solubilized in 10 mM sodium borate and 1% SDS for determination of total protein by BCA analysis (Pierce), with BSA as a standard. Content of cholesterol and ent-cholesterol was determined with a colorimetric assay based on oxidation of cholesterol with cholesterol oxidase (Cholesterol CII assay kit, Wako). Experiments with cholesterol standards showed that the color reaction reached a plateau after 5 min at 37 °C and remained stable through 60 min at this temperature. Absorbance from an equal amount of ent-cholesterol after 5 and 60 min at 37 °C was 15% and 76%, respectively, of that produced from cholesterol. The difference in time course of color development was used to determine the amounts of cholesterol and ent-cholesterol in cells. Data for content of cholesterol and ent-cholesterol were normalized to milligrams of protein and expressed as percent control.

Data Analysis. Data are reported as mean values ± SEM, with the number of replicates for each point as described in figure captions. Pairs were compared by Student's *t* test (*37*). Values of $p \leq 0.05$ were considered significant.

RESULTS

Localization of Pgp in Membrane Fractions. To determine the distribution of Pgp in membrane fractions, total cell lysates were separated on a discontinuous sucrose gradient. We used a detergent-free method (*32*) for lysing and fractionating cells to exclude the possibility that membrane-bound Pgp is redistributed in the presence of detergent (*38*, *39*). Localization of Pgp in different fractions was determined by Western blotting with mAb C219 in cells that express Pgp endogenously, through drug selection, or by transfection. Fraction 1 represents the top of the gradient, the interface of the 5% and 35% sucrose layers is collected in fraction 4, and the bottom of the gradient is in fraction 10. As previously described for this procedure, low-density membranes are expected to be present at or near the interface of the 5% and 35% solutions of sucrose (*32*). In HepG2 cells that endogenously express low levels of Pgp, the protein localized predominantly to fraction 4, and a smaller amount of Pgp was detected in fraction 5 (Figure 1A). Preliminary experiments with HepG2 cells showed that Pgp could not be detected in fractions 1−3 above the interface of 5% and 35% sucrose layers, so only fractions from this interface and below it in the gradient were analyzed routinely. Similar localization of Pgp was observed in CHO cells, which express class I Pgp endogenously, and KB 8-5 cells, which express a modest amount of *MDR1* due to selection in colchicine (Figure 1B). Conversely, NIH 3T3 cells that have been transfected with *MDR1* express very high levels of Pgp. Western blotting of fractions from these cells revealed large amounts of Pgp in fractions 3 and 10, although the protein was identified throughout the gradient in fractions 3−10 and the insoluble pellet (Figure 1B). These data suggest that Pgp is found predominantly in low-density membrane domains in cells that express physiologic amounts of the protein and that Pgp localizes to membrane fractions with higher density only when greatly overexpressed. These data are consistent with results reported previously for fractionation of Pgp on sucrose gradients (*26*, *27*).

Low-density membrane domains are enriched in glycosphingolipids, gangliosides, sphingomyelin, and cholesterol (reviewed in refs *9* and *28*). The structure of these domains can be disrupted by removal of cholesterol (*40*, *41*), shifting resident proteins to higher density fractions on sucrose gradients (*32*, *42*). To determine effects of cholesterol depletion on fractionation of Pgp, we treated cells with CD, an agent that removes cholesterol from intact cells (*43*, *44*). Cellular cholesterol was reduced to approximately 40−60% of control in all cell types after incubation with 15 mM CD for 30 min (Table 1), and content of cholesterol in these cell lines was not reduced further by incubation up to 60 min with CD (data not shown). Furthermore, no significant or consistent differences were observed in baseline content of cholesterol or extent of depletion between Pgp-expressing or nonexpressing cells. After treatment with 15 mM CD for 30 min, cells were lysed and separated on sucrose gradients. For all cell lines, the fractions in which Pgp was detected shifted to higher density following depletion of cholesterol.

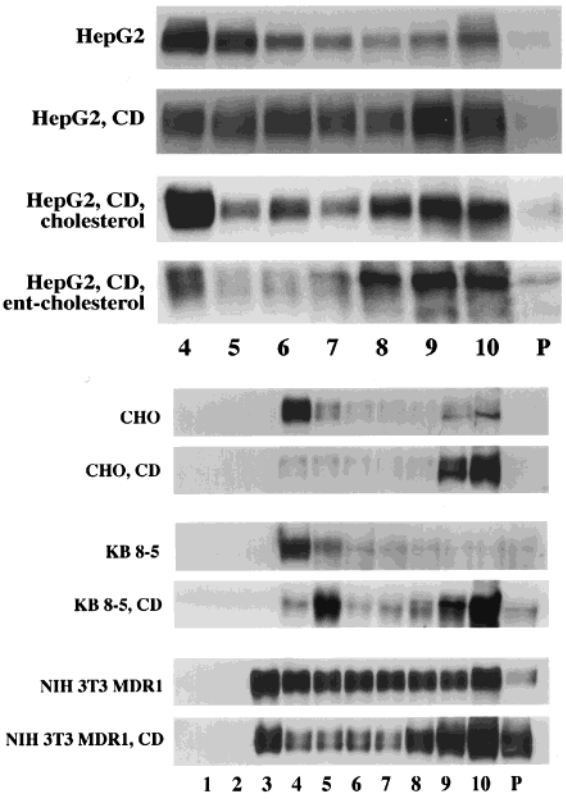

FIGURE 1: Localization of Pgp in membrane fractions in response to cholesterol depletion and repletion. HepG2 (A, top panel), CHO, KB 8-5, and NIH 3T3 MDR1 (B, bottom panel) cell lines were cultured as described under Materials and Methods. Cells were incubated in medium in the absence or presence of 15 mM cyclodextrin (CD) for 30 min at 37 °C in a 5% CO_2 incubator. HepG2 cells were further incubated in the presence or absence of 0.2 mM CD−cholesterol complex or CD−ent-cholesterol complex for 60 min at 37 °C. After being washed in PBS, cells were lysed and fractionated by a detergent-free method with discontinuous sucrose gradients (5%, 35%, and 40% steps). Fractions 1−10 (1.2 mL) were collected from the top of the gradient, and P represents the small resuspended pellet. For HepG2 cells, 0.8 mL of fractions 4−10 and the pellet were diluted and centrifuged to pellet membranes as described under Materials and Methods. Aliquots (100 μL) of each fraction were separated by SDS−PAGE, and Pgp was detected by Western blotting with mAb c219. Data are representative of at least two independent experiments.

In HepG2 cells, Pgp was distributed across the gradient, with relatively more protein localized to fraction 9 (Figure 1A). Pgp was detected in both fractions 9 and 10 in CHO and KB 8-5 cells, although relatively less Pgp from KB 8-5 cells was present in high-density fractions (Figure 1B). Increased amounts of Pgp also were detected at the bottom of the gradient and in the insoluble pellet when NIH 3T3 *MDR1* cells were treated with CD (Figure 1B). However, the first fraction in which Pgp was detected (fraction 3 for NIH 3T3 *MDR1* cells) did not change after depletion of cholesterol. These data demonstrate that CD effectively removes cholesterol from membrane compartments in which Pgp localizes, as evidenced by increased density of fractions that contain the protein on sucrose gradients.

To further characterize the relationship of cholesterol to fractionation of Pgp, CD complexes containing cholesterol or ent-cholesterol were used to restore sterols following depletion of cholesterol with CD pretreatment (*45*, *46*). For these experiments, we focused on HepG2 cells, a polarized cell line in which apical expression of Pgp reflects the physiologic pattern in vivo. Cells were treated with CD for 30 min to deplete cholesterol and then repleted with sterol by incubating for 60 min with 0.2 mM cholesterol or ent-cholesterol complexed with CD. As quantified by a colorimetric assay based on cholesterol oxidase, repletion with either sterol was equally effective in restoring total cellular content of cholesterol to baseline levels, reaching 108% ± 8% and 113% ± 16% of control for cholesterol and ent-cholesterol, respectively (Table 2). Following treatment with cholesterol, fractions that contained Pgp separated at low density on sucrose gradients in a distribution that was comparable to control cells (Figure 1A). Results with ent-cholesterol were similar to effects of cholesterol on fractionation of Pgp, although slightly more Pgp was detected in high-density membranes after treatment with ent-cholesterol. Overall, these data show that fractionation of Pgp on sucrose gradients is highly dependent on cholesterol and that the low density of the membrane compartment in which Pgp localizes is restored to a similar extent by either cholesterol or ent-cholesterol.

Table 1: Cholesterol Content in Cells Treated with CD[a]

cell type	15 mM CD (30 min) (% control ± SEM)
HepG2	47 ± 6
CHO	43 ± 3
KB 3-1	57 ± 5
KB 8-5	57 ± 13
8226	46 ± 3
Dox6	45 ± 2
NIH 3T3	52 ± 3
NIH 3T3 MDR1	44 ± 7

[a] Cells were plated as described under Materials and Methods and incubated in the appropriate serum-free medium without or with 15 mM CD for 30 min. Cells were washed in serum-free medium and extracted for lipids and protein as detailed under Materials and Methods. Data are expressed as percent control ± SEM ($n = 4$ for all points except KB 3-1, for which $n = 3$). Baseline values for untreated cells (μg of cholesterol/mg of protein): HepG2, 14.2 ± 0.9; CHO, 12.1 ± 1.2; KB 3-1, 16.5 ± 0.8; KB 8-5, 17.4 ± 1.1; 8226, 1.0 ± 0.03; Dox6, 0.8 ± 0.02; NIH 3T3, 17.0 ± 0.3; and NIH 3T3 MDR1, 27.9 ± 0.8.

Localization of Pgp and Cholesterol by Fluorescence Microscopy. To determine if acute changes in membrane content of cholesterol affect cellular localization of Pgp, intact cells were analyzed by immunofluorescence microscopy. Under baseline conditions, Pgp in HepG2 cells was detected at bile canaliculi (Figure 2A) (*47*). Following treatment with CD, Pgp retained an apical distribution, although a small amount of dispersion away from bile canaliculi was observed in some cells (Figure 2B). In nonpolar KB 8-5 (Figure 2C) and CHO cells (data not shown), Pgp localized to the plasma membrane, and this distribution was not affected by treatment with CD for 30 min (Figure 2D and data not shown). We also evaluated effects of depleting and restoring cholesterol on morphology of intact cells. Consistent with results of fractionation experiments, HepG2 cells treated with CD followed by CD−cholesterol or CD−ent-cholesterol appeared normal and indistinguishable by light microscopy as well as by fluorescence microscopy with filipin, a cholesterol-binding antibiotic (*48*) (data not shown). Overall, while treatment with CD shifted the fraction in which Pgp was detected on sucrose gradients, there was no evidence of significant relocalization of the protein within intact cells.

Table 2: Sterol Content in Cells Treated with CD Complexed with Cholesterol or Ent-cholesterol[a]

cell type	0.2 mM CD−cholesterol (60 min) (% control ± SEM)	0.2 mM CD−ent-cholesterol (60 min) (% control ± SEM)	15 mM CD (30 min), 0.2 mM CD−cholesterol (60 min) (% control ± SEM)	15 mM CD (30 min), 0.2 mM CD−ent-cholesterol (60 min) (% control ± SEM)
HepG2	122 ± 5	138 ± 3	108 ± 8	113 ± 16
CHO	ND[b]	ND	109 ± 12	117 ± 9
KB 8-5	142 ± 4	152 ± 20	111 ± 11	104 ± 9

[a] Cells were plated as described under Materials and Methods. For de novo loading with sterols, cells were incubated in appropriate serum-free medium containing 0.2 mM CD−sterol complexes for 60 min. For sequential depletion of cholesterol and replacement with sterol, cells were incubated with CD for 30 min, washed with medium, and then incubated with 0.2 mM CD-sterol for 60 min. Lipids and protein were extracted and quantified as detailed under Materials and Methods. Data are expressed as percent control ± SEM ($n = 4$). [b] Not determined.

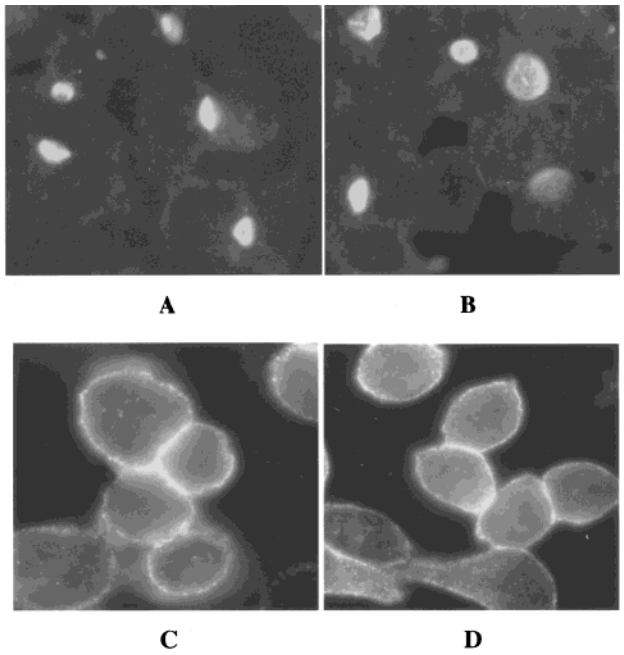

FIGURE 2: Localization of Pgp in HepG2 (A, B) and KB 8-5 (C, D) cells in response to cholesterol depletion. Cells were plated on glass cover slips and cultured for 3 days in serum-containing medium. Cells were washed and then incubated for 30 min in DMEM without (A, C) or with (B, D) 15 mM CD. Cells were processed for immunofluorescence microscopy as described under Materials and Methods, with mAb C219 and a fluorescein-conjugated secondary antibody. In HepG2 cells, fluorescence corresponds to bile canaliculi formed between adjacent cells, while fluorescence in KB 8-5 cells is predominantly localized to plasma membranes. Panels are representative of several fields from two independent experiments.

Effects of Cholesterol on Function of Class I Pgp As Probed with Tc-Sestamibi. To determine if acute changes in membrane content of cholesterol affect function of class I Pgp, we disrupted low-density membrane domains by depleting cellular cholesterol with CD as above and performed tracer assays. Cells were treated with 15 mM CD for 30 min and then incubated for an additional 30 min with Tc-Sestamibi, a transport substrate for class I Pgp (*49*). As described above, this protocol reduced cellular cholesterol to 40−60% of control in all cell lines tested. In KB 3-1 cells, which do not express *MDR1* Pgp by Western blot or functional analysis (*35*), cell contents of Tc-Sestamibi were 122 ± 7 and 315 ± 10 fmol (mg of protein)$^{-1}$ (nM_o)$^{-1}$ before and after exposure to CD, respectively ($n = 4$, representative of three independent experiments). By comparison, treatment of Pgp-expressing KB 8-5 cells with CD increased accumulation of Tc-Sestamibi from 1.8 ± 0.3 to 4.5 ± 0.2 fmol (mg of protein)$^{-1}$ (nM_o)$^{-1}$ ($n = 4$, representative of three independent experiments). Cell content of Tc-Sestamibi is inverse to expression of Pgp (*30*), thus accounting for differences in absolute accumulation of radiotracer between KB 3-1 and 8−5 cell lines. However, content of radiotracer in both cell lines increased by approximately 2.5-fold after depletion of cholesterol with CD. To confirm that these results were not unique to KB cells, we also measured cell-associated Tc-Sestamibi in 8226 and Dox6 myeloma cells, which express nonimmunodetectable and modest levels of Pgp, respectively (*18*). Net accumulation of Tc-Sestamibi in 8226 cells was 133 ± 2 fmol (mg of protein)$^{-1}$ (nM_o)$^{-1}$ under baseline conditions and increased to 242 ± 9 fmol (mg of protein)$^{-1}$ (nM_o)$^{-1}$ following treatment with CD ($n = 4$). Content of radiotracer in Dox6 cells was 2.6 ± 0.4 and 6.1 ± 0.8 fmol (mg of protein)$^{-1}$ (nM_o)$^{-1}$ ($n = 4$) without and with depletion of cholesterol. These values correspond to 1.8- and 2.3-fold increases in cell content of Tc-Sestamibi after treatment with CD in 8226 and Dox6 cells, respectively. Although *x*-fold increases in Tc-Sestamibi were slightly higher in Dox6 cells, this small difference is not proportional to the large difference in functional *MDR1* Pgp between the myeloma cell lines. By comparison, incubation with a saturating dose of GF120918, a specific inhibitor of class I Pgp (*50*), increased cell content of Tc-Sestamibi by approximately 65- and 50-fold in KB 8-5 and Dox6 cells, respectively. Accumulation of radiotracer in Pgp-negative KB 3-1 and 8226 cells was not affected by GF120918.

We also quantified accumulation of Tc-Sestamibi in parental NIH 3T3 cells and 3T3 cells transfected with *MDR1* Pgp. These cells express low and high levels of class I Pgp, respectively (Figure 1; *18*). Accumulation of radiotracer in parental 3T3 cells was 46 ± 7 fmol (mg of protein)$^{-1}$ (nM_o)$^{-1}$ ($n = 4$) but was only 1.3 ± 0.4 fmol (mg of protein)$^{-1}$ (nM_o)$^{-1}$ ($n = 4$) in fibroblasts transfected with *MDR1*. As shown in Figure 1, most Pgp in the transfected fibroblasts is not confined to low-density membranes. However, overexpression of *MDR1* Pgp still decreased accumulation of Tc-Sestamibi by approximately 35-fold compared with the parental cell line, suggesting that Pgp retains function when present in membranes with high density. Cell-associated radiotracer increased by 1.2- and 1.8-fold ($n = 4$) in parental 3T3 cells and *MDR1* transfectants, respectively, following depletion of cholesterol with CD. Similar to the myeloma cell lines, these small differences in accumulation of radiotracer are disproportionate to the large effects on accumulation of Tc-Sestamibi mediated by class I Pgp.

In the absence of class I Pgp, Tc-Sestamibi concentrates within cells in response to plasma and mitochondrial membrane potentials (*51*). Depolarizing mitochondria with carbonyl cyanide *m*-chlorophenylhydrazone (5 μM) reduced

cell content of Tc-Sestamibi to nearly background levels independent of treatment with CD (data not shown), showing that CD was not causing nonspecific binding of radiotracer to cells. Thus, the reproducible, small increases in cell content of Tc-Sestamibi following depletion of cholesterol are much less than seen with specific inhibitors of *MDR1* Pgp (*18*) and may be due to effects on membrane potential or permeability of membranes to Tc-Sestamibi. Yet, the same treatment with CD significantly changes fractionation of Pgp on sucrose gradients. Given that the effects of CD are nonspecific and small compared with specific inhibition of class I Pgp, the data indicate that short-term depletion of cholesterol in murine and human cell lines does not significantly affect function of class I Pgp as probed with Tc-Sestamibi.

Because changes in the lipid environment do not uniformly alter interactions of drugs with Pgp (*25*), we analyzed effects of specific inhibitors of *MDR1* Pgp on accumulation of Tc-Sestamibi, without or with depletion of cholesterol. HepG2 cells were incubated in medium alone or in medium containing15 mM CD for 30 min before treatment with increasing concentrations of GF120918 (Figure 3A). In the absence of GF120918, treatment with CD increased cell content of Tc-Sestamibi by 1.6-fold. Accumulation of Tc-Sestamibi increased with increasing concentrations of GF120918, reaching a plateau at 100 or 300 nM in the absence or presence of CD, respectively. We previously have observed maximal inhibition of Pgp within this range of concentrations in other cells (*35, 52*). At concentrations greater than 300 nM GF120918, content of radiotracer decreased slightly in cells not treated with CD, possibly due to toxicity. Throughout the concentration curve, absolute content of Tc-Sestamibi was greater in HepG2 cells that were treated with CD. However, when data were normalized to account for the effect of CD alone, fold increases in Tc-Sestamibi at concentrations up to 100 nM GF120918 were independent of cholesterol content of cells. Only at higher concentrations of GF120918 were *x*-fold increases in radiotracer greater in cells treated with CD, but this was due in part to decreases in content of Tc-Sestamibi in cells treated only with GF120918.

We also determined effects of disrupting low-density membrane domains in HepG2 cells on inhibition of *MDR1* Pgp by LY335979, another high-potency modulator (*53*). After depletion of cholesterol with CD, cells were incubated with Tc-Sestamibi in the absence or presence of increasing concentrations of LY335979 (Figure 3B). Independent of CD, the cell content of radiotracer reached steady state at 100 nM LY335979 and did not decrease significantly at higher concentrations of drug. Accumulation of Tc-Sestamibi, measured as femtomoles (milligram of protein)$^{-1}$ $(nM_o)^{-1}$, was greater in HepG2 cells treated with CD than control cells. Similar to data with GF120918, increased content of Tc-Sestamibi was due to additive effects of CD and LY335979 on accumulation of radiotracer. When data were normalized for the effect of CD alone, inhibition of *MDR1* Pgp by LY335979 was independent of cholesterol content of cells. Control experiments showed that localization of Pgp in low-density membranes on sucrose gradients was not affected by 30-min incubations with 300 nM of either LY335979 or GF120918 alone (data not shown).

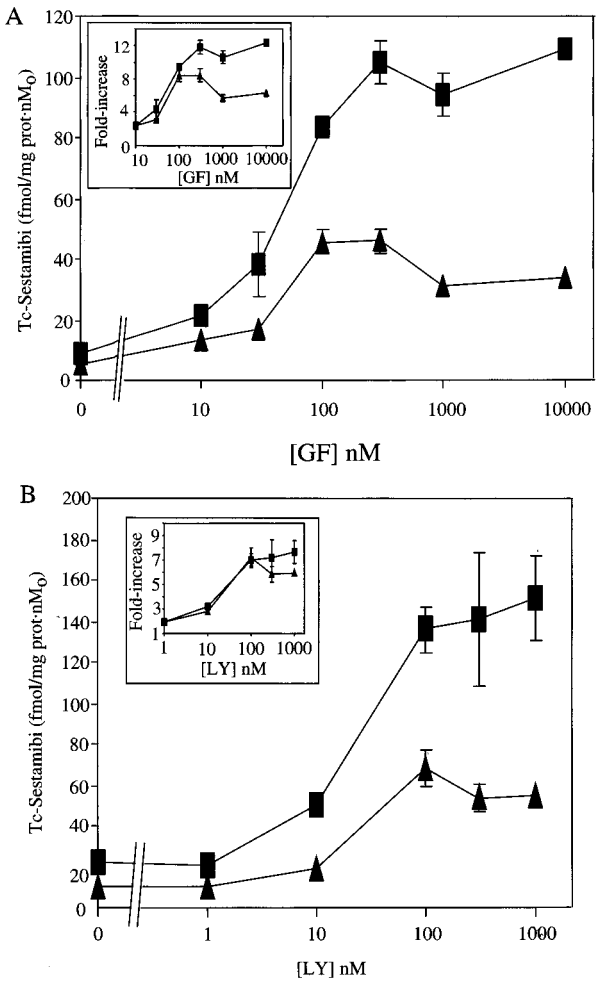

FIGURE 3: Effects of specific inhibitors of class I Pgp on [^{99m}Tc]-Sestamibi accumulation in response to cholesterol depletion in HepG2 cells. HepG2 cells were cultured as described under Materials and Methods. Cells were incubated in medium in the absence (■) or presence (□) of 15 mM CD as described in Figure 1. After being washed with MEBSS, cells were incubated with [^{99m}Tc]Sestamibi in MEBSS containing various concentrations of GF120918 (GF) (A, top panel) or LY335979 (LY) (B, bottom pane) for 30 min at 37 °C. Net cell content of Tc-Sestamibi was quantified as described under Materials and Methods. The inset to both panels shows *x*-fold increases in Tc-Sestamibi at various concentrations of modulator in the absence or presence of CD, normalized for the effect of CD alone. Each data point represents the mean of three determinations, and bars represent ±SEM when larger than the symbol. Data are representative of two (A) or one (B) independent experiment(s).

To extend these observations, we evaluated effects of cholesterol depletion and specific inhibitors of class I Pgp on accumulation of Tc-Sestamibi in other cell lines. In Pgp-negative KB 3-1 cells, content of radiotracer was not affected by concentrations of GF120918 or LY335979 up to 1 μM, independent of treatment with CD (data not shown). However, cell-associated Tc-Sestamibi increased by approximately 20-fold in KB 8-5 cells after incubation with 300 nM GF120918, a dose at which maximal inhibition of *MDR1* Pgp occurs in this cell line (Figure 4A) (*35*). The *x*-fold increase due to GF120918 alone was not significantly different in cells depleted of cholesterol. Treatment with the combination of CD and GF120918 increased cell-associated Tc-Sestamibi by approximately 23-fold over the increase mediated by CD alone. Thus, data from KB 8-5 cells are similar to those from HepG2 cells, since sequential treatment

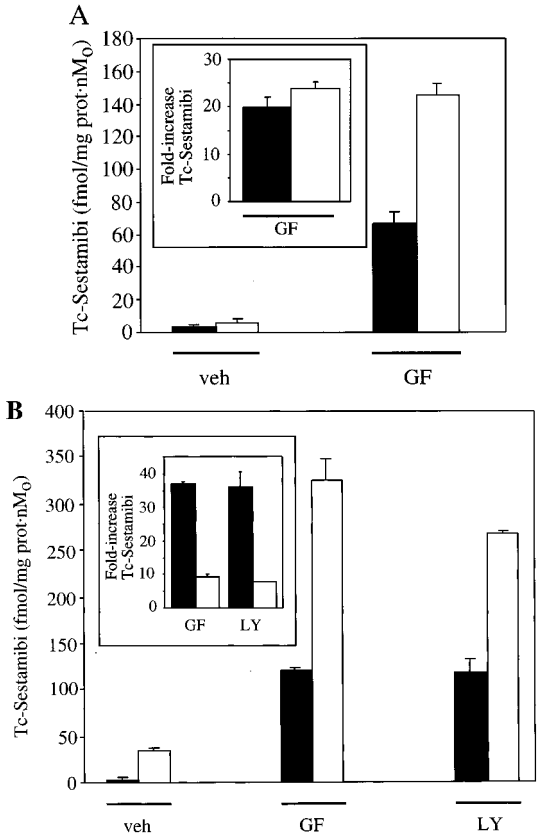

FIGURE 4: Effects of specific inhibitors of class I Pgp on [^{99m}Tc]-Sestamibi accumulation in response to cholesterol depletion in KB 8-5 and CHO cells. KB 8-5 (A, top panel) and CHO (B, bottom panel) cell lines were cultured as described under Materials and Methods. Cells were incubated in the absence (solid bars) or presence (open bars) of 15 mM CD as described in the legend to Figure 1. Cells were washed with MEBSS and incubated for 30 min at 37 °C with [^{99m}Tc]Sestamibi in MEBSS containing vehicle (veh), 300 nM GF120918 (GF), or 300 nM LY335979 (LY). The inset to both panels shows *x*-fold increases in Tc-Sestamibi accumulation with GF120918 or LY335979 in the absence or presence of CD, normalized to the effect of CD alone. Each column represents the mean of four determinations; bars represent +SEM. Data from each cell line are representative of at least two independent experiments.

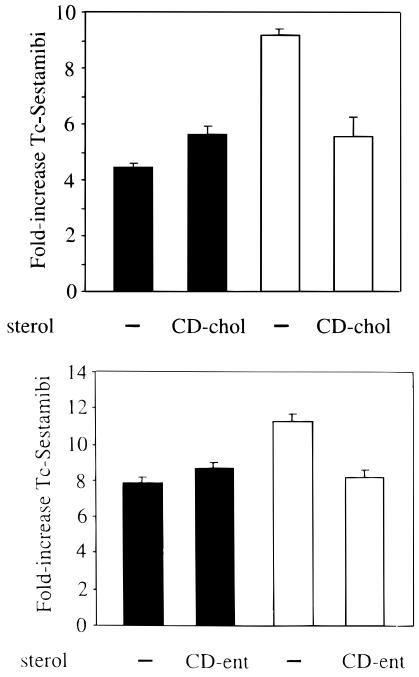

FIGURE 5: Effects of GF120918 on [^{99m}Tc]Sestamibi accumulation in response to cholesterol depletion and repletion in HepG2 cells. HepG2 cells were cultured as described under Materials and Methods. The cells were incubated in the absence (solid bars) or presence (open bars) of 15 mM CD as described in the caption to Figure 1. Cells were then washed with medium and incubated in the absence (−) or presence of 0.2 mM CD−cholesterol complex (CD-chol) (A, top panel) or CD−ent-cholesterol complex (CD-ent) (B, bottom panel) for 60 min at 37 °C. This was followed by a 30-min incubation in MEBSS containing [^{99m}Tc]Sestamibi and 300 nM GF120918 (GF). Each column represents the mean of four determinations; bars represent + SEM. Data are representative of two independent experiments.

with CD and GF120918 produced no additive effects on *x*-fold accumulation of radiotracer.

To characterize interactions of specific inhibitors and cholesterol in a hamster cell line with endogenous expression of class I Pgp, we quantified accumulation of Tc-Sestamibi in CHO cells. Content of Tc-Sestamibi in these cells increased by approximately 10-fold after treatment with CD (Figure 4B), which was significantly greater than the other cell lines; the mechanisms underlying this difference are uncertain. Cells treated sequentially with CD and a saturating dose of either GF120918 or LY335979 had a greater content of radiotracer than cells incubated with only one of the specific modulators. Unlike human HepG2 or KB 8-5 cells, effects of either GF120918 or LY335979 on class I Pgp in CHO cells were dependent on cholesterol content. Incubation with either specific inhibitor alone increased accumulation of Tc-Sestamibi by approximately 36-fold over cells treated with vehicle. Following depletion of cholesterol with CD, treatment of CHO cells with GF120918 or LY335979 enhanced cell-associated radiotracer by only 8−9-fold above that observed with CD alone. Similar to HepG2 cells, fractionation of Pgp on sucrose gradients was not altered by incubation of CHO cells with 300 nM of either GF120918 or LY335979 for 30 min (data not shown). In summary, these data show that interactions of specific inhibitors, cholesterol, and class I Pgp are dependent on cell type. At least in CHO cells, these drugs are significantly less effective inhibitors of class I Pgp after use of CD to remove cholesterol and disrupt low-density membrane domains.

To determine if CD was disrupting enantiospecific interactions between cholesterol, *MDR1* Pgp, and a specific inhibitor, we used different combinations of CD and repletion of cellular cholesterol with either cholesterol or ent-cholesterol before incubation with GF120918 in HepG2 cells. As a baseline, cell content of Tc-Sestamibi following incubation with 300 nM GF120918 increased by 4.4-fold relative to vehicle control (Figure 5A). In the absence of cholesterol depletion, cells loaded with 0.2 mM cholesterol complexed with CD for 1 h increased total cholesterol to 122% ± 5% of control (Table 2), but this treatment only minimally enhanced accumulation of radiotracer above that seen with GF120918 alone. Sequential incubations with CD and GF120918 produced the expected additive increase in cell content of Tc-Sestamibi, and the effect of CD on accumulation of Tc-Sestamibi was nearly completely reversed by using 0.2 mM cholesterol complexed with CD. Parallel experiments with ent-cholesterol showed effects that were essentially the same as those observed with cholesterol, although *x*-fold increases in accumulation of Tc-Sestamibi

differed between experiments (Figure 5B). Use of 0.2 mM ent-cholesterol−CD increased total cellular cholesterol (cholesterol and ent-cholesterol) to 138% ± 3% of control (Table 2). As observed in cells loaded with cholesterol, sequential treatment with ent-cholesterol and GF120918 resulted in slightly greater accumulation of Tc-Sestamibi than in cells incubated only with the specific inhibitor of *MDR1* Pgp. Similarly, use of ent-cholesterol to restore cell sterol after incubation with CD returned cell-associated radiotracer to levels equivalent to those of cells treated with GF120918 alone. Interchangeable effects of cholesterol and ent-cholesterol on cell content of Tc-Sestamibi also were seen in nonpolar KB 8-5 cells (data not shown). Overall, these data show that function and inhibition of *MDR1* Pgp as probed with Tc-Sestamibi do not depend on enantiospecific interactions with cholesterol.

Effects of Cholesterol on Function of Class I Pgp As Probed with Daunomycin. To further analyze effects of cholesterol on class I Pgp, we also used daunomycin as a probe for transport activity mediated by Pgp. Although both Tc-Sestamibi and daunomycin are hydrophobic, cationic substrates for Pgp, the latter drug also has a titratable proton, which has been postulated to induce accumulation within acidic compartments in cells (*54*). Paired cell lines that differ in expression of *MDR1* Pgp were depleted of cholesterol with CD as described above and then incubated with daunomycin for 30 min. In KB 3-1 cells, treatment with CD did not significantly affect accumulation of daunomycin. Cell content of daunomycin was 740 ± 54 and 707 ± 23 pmol (mg of protein)$^{-1}$ (μM_o)$^{-1}$ without and with CD, respectively (n = 4, representative of two independent experiments). Conversely, depletion of cholesterol increased net cell content of daunomycin in KB 8-5 cells by approximately 1.5-fold, from 161 ± 21 to 248 ± 11 μmol (mg of protein)$^{-1}$ (M_o)$^{-1}$ (n = 4, representative of two independent experiments) ($p < 0.05$). In 8226 myeloma cells, depletion of cholesterol with CD increased accumulation of daunomycin from 15.5 ± 1.1 to 21.2 ± 1.9 pmol (mg of protein)$^{-1}$ (μM_o)$^{-1}$, which represents a 1.6-fold change (n = 6). A 1.6-fold increase in net content of daunomycin also was observed in Pgp-expressing Dox6 cells; cell-associated daunomycin was 7.5 ± 0.8 and 12.2 ± 2.2 pmol (mg protein)$^{-1}$ (μM_o)$^{-1}$ in the absence and presence of CD, respectively (n = 6). Overall, these data show that disruption of low-density membrane domains through depletion of cholesterol has cell-type-specific effects on accumulation of daunomycin and does not consistently target cells that express *MDR1* Pgp.

To further characterize interactions of cholesterol and specific inhibitors of class I Pgp, we measured net content of daunomycin in cells treated with differing combinations of CD and inhibitors. Again, we focused on cell types that endogenously express class I Pgp. In HepG2 cells, CD treatment before incubation with daunomycin was more effective at enhancing cell content of radiotracer than saturating doses of either GF120918 or LY335979 (Figure 6A). Increases in accumulation of daunomycin were 1.6-, 1.3-, and 1.1-fold for CD, GF120918, and LY335979, respectively. Combined treatment of HepG2 cells with CD and either inhibitor did not increase accumulation of daunomycin more than CD alone. To determine if these effects of cholesterol depletion were unique to HepG2 cells, we repeated this experiment in CHO cells. In this cell line,

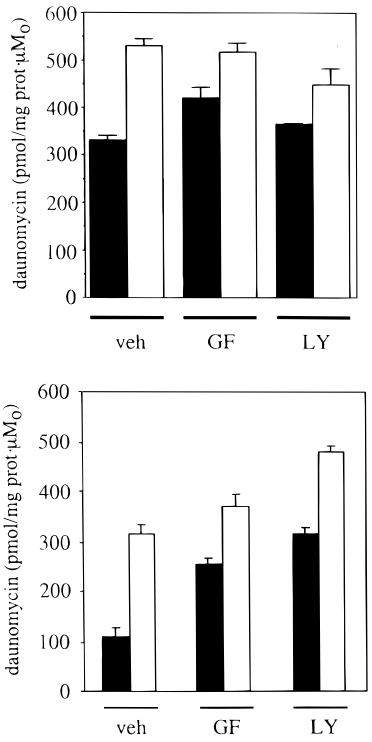

FIGURE 6: Effects of specific inhibitors of class I Pgp on [^{3}H]-daunomycin accumulation in response to cholesterol depletion in HepG2 and CHO cells. HepG2 (A, top panel) and CHO (B, bottom panel) cell lines were cultured as described under Materials and Methods. Cells were incubated in the absence (solid bars) or presence (open bars) of 15 mM CD as described in Figure 1. Cells were washed with MEBSS followed by a 30-min incubation with [^{3}H]daunomycin in MEBSS containing vehicle (veh), 300 nM GF120918 (GF), or 300 nM LY335979 (LY). Each column represents the mean of three determinations; bars represent + SEM. Data are representative of two (A) or one (B) independent experiment(s).

increases in accumulation of daunomycin were 2.8-, 2.3-, and 2.8-fold above control after treatment with CD, GF120918, or LY335979, respectively (Figure 6B). Unlike HepG2 cells, cell-associated daunomycin in CHO cells was significantly greater following sequential treatment with CD and either GF120918 or LY335979 compared with CD alone. Increases in daunomycin after cholesterol depletion and incubation with a specific inhibitor were 3.3- and 4.3-fold for GF120918 ($p < 0.05$) and LY335979 ($p < 0.005$), respectively.

We then used either cholesterol or ent-cholesterol to replace sterols in cells after treatment with CD. HepG2 cells were incubated with CD and then with 0.2 mM CD−cholesterol complex to restore total cholesterol to baseline levels as described above. Under these conditions, accumulation of daunomycin was the same as in control cells (Figure 7A). However, content of daunomycin in HepG2 cells was significantly less than control when cellular sterols were replaced with ent-cholesterol ($p < 0.005$). Similar differences between cholesterol and ent-cholesterol also were observed in CHO cells (Figure 7B). Following treatment with CD, restoring cellular sterols with cholesterol partially reversed the effect of CD on accumulation of daunomycin, returning content of radiotracer to 1.5-fold above control. By comparison, CHO cells incubated with ent-cholesterol had less cell-associated daunomycin than control cells ($p < 0.05$). Thus, these data show that accumulation of daunomycin is

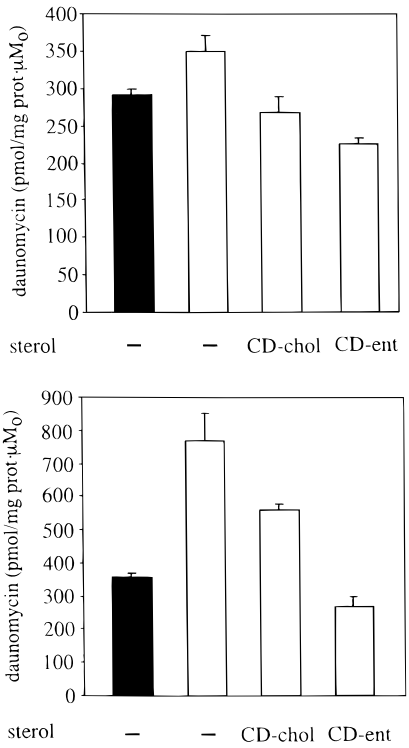

FIGURE 7: Accumulation of [^{3}H]daunomycin in HepG2 and CHO cells in response to cholesterol depletion and repletion. HepG2 (A, top panel) and CHO (B, bottom panel) cells were cultured as described under Materials and Methods. Cells were incubated in the absence (solid bars) or presence (open bars) of 15 mM CD as described in Figure 1, followed by a 60-min incubation in the absence or presence of 0.2 mM CD−sterol complexes as described in Figure 4. After being washed in MEBSS, cells were incubated for 30 min with [^{3}H]daunomycin in MEBSS. Each column represents the mean of three determinations; bars represent + SEM. Data are representative of two (A) or one (B) independent experiment(s).

affected by enantioselective interactions with cholesterol.

DISCUSSION

By use of a detergent-free protocol for fractionating cells, the data presented here demonstrate that Pgp is present in low-density membrane domains. The density of fractions that contain Pgp is partially dependent on cholesterol, and effects of cholesterol depletion are reversed to a similar extent by either cholesterol or ent-cholesterol. These data complement recent work by Lavie et al. (*26*) and Demeule et al. (*27*) on localization of Pgp in low-density membranes. Changes in position of Pgp on sucrose gradients in response to CD and CD−sterol complexes demonstrate that cholesterol can be removed and restored from membrane compartments that contain Pgp, allowing us to quantify effects of cholesterol on function and inhibition of class I Pgp in intact cells.

Depletion of cholesterol with CD showed cell-type- and substrate-dependent effects on the transport activity of class I Pgp. As probed with Tc-Sestamibi, function of *MDR1* Pgp was not affected by depletion of cholesterol. Treatment with CD caused small (2-fold) increases in cell content of Tc-Sestamibi in human and murine cell lines, independent of class I Pgp. These data are consistent with previous work showing that the chemosensitizers verapamil and reserpine potentiated cytotoxicity of drugs in the multidrug-resistance phenotype in cells that did not express class I Pgp (*55*). Effects of these chemosensitizers putatively were mediated through increases in membrane permeability to cytotoxic drugs. Further support for dissociating function of *MDR1* Pgp (as probed with Tc-Sestamibi) from membrane content of cholesterol is data obtained with NIH 3T3 *MDR1* cells. Although most Pgp in these cells is detected in high-density fractions on sucrose gradients, accumulation of radiotracer is very low compared with parental 3T3 cells. These data show that *MDR1* Pgp confers multidrug resistance transport activity even when it fractionates outside of low-density, cholesterol-rich membranes. Specific inhibitors of human *MDR1* Pgp also were not significantly affected by decreases in cholesterol and did not affect fractionation of Pgp on sucrose gradients. Moreover, effects of CD were reversed equally by either cholesterol or ent-cholesterol, demonstrating that drug transport function and inhibition of *MDR1* Pgp as assayed with Tc-Sestamibi are not affected by enantiospecific interactions with cholesterol.

In contrast, use of daunomycin as a probe showed that cell-type-specific differences exist in effects of cholesterol depletion on function of *MDR1* Pgp, although inhibition of the protein with GF120918 or LY335979 was not affected by removal of cholesterol. Differences also were observed when cholesterol was depleted with CD and then restored with either cholesterol or ent-cholesterol before incubation with daunomycin. Although total content of sterol (cholesterol or cholesterol and ent-cholesterol) returned to baseline, accumulation of daunomycin was significantly less in cells containing ent-cholesterol as compared with cells repleted with cholesterol. We cannot exclude the possibility that effects of cholesterol and ent-cholesterol on transport of daunomycin by Pgp are caused by alterations in membrane fluidity. Compounds that nonspecifically increase membrane fluidity previously have been shown to inhibit Pgp (*19*). However, enantiospecific effects on function of class I Pgp as measured with daunomycin suggest a specific interaction between cholesterol and the localized binding site for daunomycin on Pgp.

Depletion of cholesterol affected both function and inhibition of class I Pgp differently in CHO cells than in any of the cells expressing human *MDR1* Pgp or endogenous murine class I Pgp. Following treatment with CD, *x*-fold increases in accumulation of Tc-Sestamibi were comparatively greater in CHO cells than other cell lines, and specific inhibitors of class I Pgp were much less potent. Similar differences between HepG2 and CHO cells also were observed with daunomycin. In the former cell line, inhibition of *MDR1* Pgp was not altered following treatment with CD. Conversely, effects of both GF120918 and LY335979 in CHO cells were greater after depletion of cholesterol. These results suggest that isoform-specific differences exist between interactions of cholesterol with hamster or human Pgp, although the influence of other features specific to CHO cells cannot be excluded. Variations in drug resistance profiles and response to inhibitors have been reported previously among human *MDR1* and mouse *mdr1* and *mdr3* (*56*). By demonstrating that cholesterol has cell-type-specific effects on class I Pgp, our data extend prior work by Romsicki and Sharom (*25*), who determined that cholesterol affects interactions only of hamster Pgp with selected drugs.

The current study was designed to analyze acute effects of cholesterol depletion on localization and function of Pgp

under short-term steady-state conditions. Previous investigations have used agents that lower cholesterol content or bind cholesterol to determine effects of low-density membrane domains on receptors (*33*, *46*), signaling molecules (*32*), and signal transduction pathways (*57*). However, this approach does not address the function of sphingolipid−cholesterol rafts in trafficking of proteins within cells. Sorting of transmembrane proteins to apical surfaces of polarized cells or apical cognate routes of nonpolar cells preferentially uses sphingolipid−cholesterol rafts (*9*), although association with rafts is not required for trafficking of all apical membrane proteins (*58*, *59*). By immunofluorescence microscopy, Pgp localized to bile canaliculi in polarized HepG2 cells and retained an apical distribution following incubation with CD. Likewise, Pgp remained associated with the plasma membrane of nonpolar cells after depletion of cholesterol. In some HepG2 cells, the protein appeared to localize both in and adjacent to bile canaliculi, suggesting that trafficking of Pgp may be affected by depletion of cholesterol. Similar results were reported recently by Ostermeyer et al., who studied effects of CD on trafficking of a glycosylphosphatidylinositol-linked protein. Although initial delivery of the protein to the cell surface was not affected by CD, these authors suggested that rates of protein internalization and/or recycling from the cell membrane may be dependent on membrane rafts (*59*). Currently, it is unknown if Pgp requires interactions with lipid rafts for proper targeting to apical membranes in polarized cells or the equivalent membrane domains in cells without polarity. If rafts are necessary for normal trafficking of Pgp, then long-term disruption of these lipid domains could result in retention of the protein in intracellular organelles or improper targeting to basolateral membranes. Under these circumstances, long-term depletion of cholesterol potentially may have a significant effect on function of Pgp.

Fractionation of Pgp with low-density membranes also raises the possibility that the protein may localize to caveolae, which represent a subclass of low-density membranes (*60*−*62*). In drug-resistant CH^RC5 cells and brain capillaries, Pgp has been shown to coimmunoprecipitate with caveolin (*27*), an integral membrane protein that is associated with caveolae (*63*). Further investigation will be required to determine if Pgp localizes within morphologically defined caveolae and any functional consequences of such localization.

In summary, physiologic levels of Pgp fractionate in low-density membrane domains on sucrose gradients, but marked overexpression causes the protein to distribute into fractions with higher density. Density of the membrane compartment that contains Pgp responds to depletion of cholesterol or replacement with cholesterol or ent-cholesterol. However, changes in cell content of cholesterol do not significantly affect short-term, steady-state localization of Pgp in intact cells. Both depletion of cholesterol and replacement of cholesterol with ent-cholesterol showed cell-type-specific effects on the transport function of class I Pgp and potency of specific inhibitors of the protein. Overall, acute depletion of cholesterol and disruption of low-density membrane domains do not universally alter the drug transport function of class I Pgp.

REFERENCES

1. Wadkins, R., and Roepe, P. (1997) *Int. Rev. Cytol. 171*, 121−165.
2. Sharom, F. (1997) *J. Membr. Biol. 25*, 161−175.
3. Ambudkar, S., Dey, S., Hrycyna, C., Ramachandra, M., Pastan, I., and Gottesman, M. (1999) *Annu. Rev. Pharmacol. Toxicol. 31*, 361−398.
4. Johnstone, R., Ruefli, A., and Smyth, M. (2000) *Trends Biochem. Sci. 25*, 1−6.
5. van Helvoort, A., Smith, A. J., Sprong, H., Fritzsche, I., Schinkel, A. H., Borst, P., and van Meer, G. (1996) *Cell 87*, 507−517.
6. Higgins, C. F., and Gottesman, M. M. (1992) *Trends Biochem. Sci. 17*, 18−21.
7. Cordon-Cardo, C., O'Brien, J. P., Boccia, J., Casals, D., Bertino, J. R., and Melamed, M. R. (1990) *J. Histochem. Cytochem. 38*, 1277−1287.
8. Rao, V., Dahlheimer, J., Bardgett, M., Snyder, A., Finch, R., Sartorelli, A., and Piwnica-Worms, D. (1999) *Proc. Natl. Acad. Sci. U.S.A. 96*, 3900−3905.
9. Simons, K., and Ikonen, E. (1997) *Nature 387*, 569−572.
10. Van't Hof, W., and Van Meer, G. (1994) *Curr. Top. Membr. 40*, 539−563.
11. Schinkel, A., Mayer, U., Wagenaar, E., Mol, C., van Deemer, L., Smit, J., van der Valk, M., Voordouw, A., Spits, H., van Tellingen, O., Zijlmans, J., Fibbe, W., and Borst, P. (1997) *Proc. Natl. Acad. Sci. U.S.A. 94*, 4028−4033.
12. Robinson, L., Roberts, W., Ling, T., Lamming, D., Sternberg, S., and Roepe, P. (1997) *Biochemistry 36*, 11169−11178.
13. Smyth, M. J., Krasovskis, E., Sutton, V. R., and Johnstone, R. W. (1998) *Proc. Natl. Acad. Sci. U.S.A. 95*, 7024−7029.
14. Randolph, G., Beaulieu, S., Pope, M., Sugawara, I., Hoffman, L., Steinman, R., and Muller, W. (1998) *Proc. Natl. Acad. Sci. U.S.A. 95*, 6924−6929.
15. Lange, Y., and Steck, T. (1994) *J. Biol. Chem. 269*, 29371−29374.
16. Field, F., Born, E., Chen, H., Murthy, S., and Mathur, S. (1995) *J. Lipid Res. 36*, 1533−1543.
17. Debry, P., EA, N., Neklason, D., and Metherall, J. (1997) *J. Biol. Chem. 272*, 1026−1031.
18. Luker, G., Nilsson, K., Covey, D., and Piwnica-Worms, D. (1999) *J. Biol. Chem. 274*, 6979−6991.
19. Sinicrope, F. A., Dudeja, P. K., Bissonnette, B. M., Safa, A. R., and Brasitus, T. A. (1992) *J. Biol. Chem. 267*, 24995−5002.
20. Regev, R., Assaraf, Y., and Eytan, G. (1999) *Eur. J. Biochem. 259*, 18−24.
21. Callaghan, R., Berridge, G., Ferry, D., and Higgins, C. (1997) *Biochim. Biophys. Acta 1328*, 109−124.
22. Saeki, T., Shimabuku, A., Ueda, K., and Komano, T. (1992) *Biochim. Biophys. Acta 1107*, 105−110.
23. Saeki, T., Shimabuku, A. M., Azuma, Y., Shibano, Y., Komano, T., and Ueda, K. (1991) *Agric. Biol. Chem. 55*, 1859−1965.
24. Urbatsch, I. L., and Senior, A. E. (1995) *Arch. Biochem. Biophys. 316*, 135−140.
25. Romsicki, Y., and Sharom, F. (1999) *Biochemistry 38*, 6887−6896.
26. Lavie, Y., Fiucci, G., and Liscovitch, M. (1998) *J. Biol. Chem. 273*, 32380−32383.
27. Demeule, M., Jodoin, J., Gingras, D., and Beliveau, R. (2000) *FEBS Lett. 466*, 219−224.
28. Prinetti, A., Iwabuchi, K., and Hakomori, S. (1999) *J. Biol. Chem. 274*, 20916−20924.
29. Kumar, A., and Covey, D. (1999) *Tetrahedron Lett. 40*, 823−826.
30. Piwnica-Worms, D., Rao, V., Kronauge, J., and Croop, J. (1995) *Biochemistry 34*, 12210−12220.
31. Dalton, W. S., Durie, B. G. M., Alberts, D. S., Gerlach, J. H., and Cress, A. E. (1986) *Cancer Res. 46*, 5125−5130.
32. Pike, L., and Miller, J. (1998) *J. Biol. Chem. 273*, 22298−22304.
33. Klein, U., Gimpl, G., and Fahrenholz, F. (1995) *Biochemistry 34*, 13784−13793.
34. Roy, S., Luetterforst, R., Harding, A., Apolloni, A., Etheridge, M., Stang, E., Rolls, B., Hancock, J., and Parton, R. (1999) *Nat. Cell Biol. 1*, 98−105.

35. Luker, G., Rao, V., Crankshaw, C., Dahlheimer, J., and Piwnica-Worms, D. (1997) *Biochemistry 36*, 14218−14227.
36. Bosch, I., Crankshaw, C., Piwnica-Worms, D., and Croop, J. (1997) *Leukemia 11*, 1131−1137.
37. Glantz, S. A. (1987) *Primer of Biostatistics*, 2nd ed., p 379, McGraw-Hill, Inc., New York.
38. Chang, W., Ying, Y., Rothberg, K., Hooper, N., Turner, A., Gambliel, H., De Gunzburg, J., Mumby, S., Gilman, A., and Anderson, R. (1994) *J. Cell Biol. 126*, 127−138.
39. Morishima-Kawashima, M., and Ihara, Y. (1998) *Biochemistry 37*, 15247−15253.
40. Varma, R., and Mayor, S. (1998) *Nature 394*, 798−801.
41. Friedrichson, T., and Kurzchalia, T. (1998) *Nature 394*, 802−805.
42. Green, J., Zhelesnyak, A., Chung, J., Lindberg, F., Sarfati, M., Frazier, W., and Brown, E. (1999) *J. Cell Biol. 146*, 673−682.
43. Ohtani, Y., Irie, T., Uekama, K., Fukunaga, K., and Pitha, J. (1989) *Eur. J. Biochem. 186*, 17−22.
44. Kilsdonk, E., Yancey, P., Stoudt, G., Bangerter, F., Johnson, W., Phillips, M., and Rothblat, G. (1995) *J. Biol. Chem. 270*, 17250−17259.
45. Gimpl, G., Klein, U., Reilander, H., and Fahrenholz, F. (1995) *Biochemistry 34*, 13794−13801.
46. Gimpl, G., Burger, K., and Fahrenholz, F. (1997) *Biochemistry 36*, 10959−10974.
47. Zegers, M., and Hoekstra, D. (1997) *J. Cell Biol. 138*, 307−321.
48. Porn, M., and Slotte, J. (1995) *Biochem. J. 308*, 269−274.
49. Sharma, V., and Piwnica-Worms, D. (1999) *Chem. Rev. 99*, 2545−2560.
50. Hyafil, F., Vergely, C., Du Vignaud, P., and Grand-Perret, T. (1993) *Cancer Res. 53*, 4595−4602.
51. Piwnica-Worms, D., Kronauge, J., and Chiu, M. (1990) *Circulation 82*, 1826−1838.
52. Chen, W., Luker, K., Dahlheimer, J., Pica, C., Luker, G., and Piwnica-Worms, D. (2000) *Biochem. Pharmacol.* (in press).
53. Dantzig, A., Shepard, R., Cao, J., Law, K., Ehlhardt, W., Baughman, T., Bumol, T., and Starling, J. (1996) *Cancer Res. 56*, 4171−4179.
54. Altan, N., Chen, Y., Schindler, M., and Simon, S. (1998) *J. Exp. Med. 187*, 1583−1598.
55. Drori, S., Eytan, G., and Assaraf, Y. (1995) *Eur. J. Biochem. 228*, 1020−1029.
56. Tang-Wai, D., Kajiji, S., DiCapua, F., de Graaf, D., Roninson, I., and Gros, P. (1995) *Biochemistry 34*, 32−39.
57. Liu, J., Oh, P., Horner, T., Rogers, R., and Schnitzer, J. (1997) *J. Biol. Chem. 272*, 7211−7222.
58. Zheng, X., Lu, D., and Sadler, J. (1999) *J. Biol. Chem. 274*, 1596−1605.
59. Ostermeyer, A., Beckrich, B., Ivarson, K., Grove, K., and Brown, B. (1999) *J. Biol. Chem. 274*, 34459−34466.
60. Schnitzer, J., McIntosh, D., Dvorak, A., Liu, J., and Oh, P. (1995) *Science 269*, 1435−1439.
61. Harder, T., and Simons, K. (1997) *Curr. Opin. Cell Biol. 4*, 534−542.
62. Brown, D., and London, E. (1998) *J. Membr. Biol. 164*, 103−114.
63. Anderson, R. (1998) *Annu. Rev. Biochem. 67*, 199−225.

BI9928593